

Article

Genome-Wide Characterization of *Solanum tuberosum* CCoAOMT Gene Family and Identification of StCCoAOMT Genes Involved in Anthocyanin Biosynthesis

Yaxuan Peng [†], Suao Sheng [†], Tongtong Wang, Jiafeng Song, Daijuan Wang, Yixuan Zhang, Jielan Cheng, Tingting Zheng, Zhaoyan Lv, Xiaobiao Zhu and Hualan Hou ^{*}

School of Horticulture, Anhui Agricultural University, Hefei 230036, China

^{*} Correspondence: hhl@ahau.edu.cn

[†] These authors contributed equally to this work.

Abstract: Background: The caffeoyl-CoA-O methyltransferase (CCoAOMT) family plays essential roles in the methylation of various secondary metabolites, including anthocyanins. Despite the wide identification of the CCoAOMT family in plants, the characterization and function of CCoAOMT protein members in *Solanum tuberosum* remain poorly understood. Methods and Results: In this study, a total of 12 StCCoAOMT members were identified in the genome of *S. tuberosum* using the Blastp and HMM search and were unevenly located on eight chromosomes. Collinearity analysis revealed that four tandem duplicated gene pairs and two segmental duplicated gene pairs existed in the *S. tuberosum* genome, demonstrating that duplication events play a key role in the expansion of the CCoAOMT family. All StCCoAOMTs were clustered into group I and group II based on phylogenetic analysis, which was further verified by the conserved motifs and gene structures analysis. The *cis*-acting elements analysis illustrated that StCCoAOMTs might be important for photosynthesis, hormone responses, and abiotic stress. Expression analysis demonstrated that StCCoAOMT genes have diverse transcript levels in various tissues and that StCCoAOMT10 was significantly expressed in purple potatoes with abundant anthocyanin content according to RNA-seq data and qRT-PCR assays. In addition, the subcellular localization assay validated that the StCCoAOMT10 protein was mainly localized in the cytoplasm and nucleus. Conclusions: These results will be of great importance for a better understanding of the features of CCoAOMT family members, especially of the candidate genes involved in the methylation of anthocyanins in *S. tuberosum*, and also for improving the nutritional quality of *S. tuberosum*.

Keywords: caffeoyl-CoA-O methyltransferase; expression pattern; functional analysis; StCCoAOMT10; subcellular localization



Citation: Peng, Y.; Sheng, S.; Wang, T.; Song, J.; Wang, D.; Zhang, Y.; Cheng, J.; Zheng, T.; Lv, Z.; Zhu, X.; et al. Genome-Wide Characterization of *Solanum tuberosum* CCoAOMT Gene Family and Identification of StCCoAOMT Genes Involved in Anthocyanin Biosynthesis. *Genes* **2024**, *15*, 1466. <https://doi.org/10.3390/genes15111466>

Academic Editor: Zhiqiang Wu

Received: 17 October 2024

Revised: 9 November 2024

Accepted: 10 November 2024

Published: 13 November 2024



Copyright: © 2024 by the authors. Licensee MDPI, Basel, Switzerland. This article is an open access article distributed under the terms and conditions of the Creative Commons Attribution (CC BY) license (<https://creativecommons.org/licenses/by/4.0/>).

1. Introduction

S. tuberosum, as the fourth largest staple crop in the world, followed by *Oryza sativa*, *Zea mays*, and *Triticum aestivum*, plays an important role in ensuring global food security [1,2]. Potato plants contain a variety of secondary metabolites, including lignin and flavonoids. Lignin mainly synthesizes in secondary thickening cells and plays a mechanical support role for plant cells and tissues, contributing to the transportation of nutrients and water [3]. Lignin has been widely studied in a range of plants because it is a crucial product of the phenylalanine metabolism pathway. Flavonoids are a class of polyphenol compounds in plants that play various roles in plant biological processes such as organ development, plant coloration, abiotic stress response, and hormone transport [4,5]. For example, shade plants, which are rich in kaempferol and/or apigenin derivatives, have the characteristics of large leaf lamina, a long internode, and decreased leaf thickness [6]. Quercetin 3-O-rutinoside (rutin) may enhance membrane rigidity by interacting with the polar head of phospholipids at the lipid–water interface, thereby protecting membranes from oxidative damage [7]. The

flavonol compounds play specific roles in UVB tolerance [8,9]. Furthermore, several studies have indicated that flavonoids are responsible for an array of therapeutic potential in humans, such as cancer, diabetes, and cardiovascular diseases [10]. For instance, quercetin and its derivatives were used for the treatment of osteoporosis due to their natural antioxidant properties [11,12]. Anthocyanins play important roles in repressing the reproduction of cell lines for human stomach cancer, prostate cancer, and erythrocyte leukemia [13].

Anthocyanins derived from the flavonoid pathway play essential roles in flower and fruit pigmentation, plant development, pollination and seed dispersal, herbivore and pathogen defense, and stress response [14,15]. For example, delphinidin-based derivatives, which were ubiquitously detected in the purple fruits of *Solanum lycopersicum*, *Solanum melongena*, and *Capsicum annuum*, are considered the main reason for the formation of fruit colors [16]. At present, large numbers of anthocyanins have been identified in plants, and six common anthocyanins widely exist in potato tubers, namely, pelargonidin, cyanidin, delphinidin, peonidin, malvidin, and petunidin. Among them, pelargonidin is the predominant anthocyanin in red potato tubers, while petunidin is the main anthocyanin in purple potato tubers [16–18]. The biosynthesis of anthocyanins includes acetylation, glycosylation, and O-methylation at different positions of the flavonoid skeleton (e.g., naringenin). Methylation modification is proposed to modify the water solubility of anthocyanins and improve their stability, thus significantly promoting the accumulation of color [19–21]. Anthocyanin metabolism is regulated by many factors, including genetic, developmental, and environmental conditions. In terms of genetic regulation, the induction or closing of anthocyanin biosynthesis depends on the transcript abundance of the regulatory and structural genes in plants [16]. Among them, structural genes encode the enzymes that catalyze each reaction step, including *CHS*, *CHI*, *F3H*, *F3'H*, *F3'5'H*, *DFR*, *ANS*, *3GT*, *AT*, and *OMT*, while regulatory genes encode transcription factors controlling the expression of the structural genes, such as MYB, basic helix–loop–helix (bHLH), and the WD40 repeat protein [22,23].

O-methyltransferases (OMTs) are various groups of multifunctional enzymes that play a crucial role in regulating several secondary metabolic processes, including lignin and flavonoid biosynthesis [24,25]. Plant OMTs were divided into two primary families according to their enzymatic properties and molecular weight: the caffeic acid O-methyltransferase (COMT) family with subunit sizes of 38–42 kDa and the Mg²⁺-dependent caffeoyl coenzyme A O-methyltransferase (CCoAOMT) family with low subunit sizes of 26–30 kDa [26,27]. Numerous studies have shown that the COMT subfamily plays important roles in lignin, melatonin, and flavonoid biosynthesis [28–33]. For instance, the *CitOMT2* gene was verified as flavonoid 8-O-methyltransferase in vitro [34]. The overexpression of *COMT1* contributes to melatonin biosynthesis in tomato plants [35]. The CCoAOMT family acts as a key enzyme that participates in lignin biosynthesis and plays a vital role in converting the Caffeoyl-CoA into Feruloyl-CoA in plants [36]. CCoAOMT proteins possess a complete AdoMet MTases domain and comprise eight conserved motifs designated as A to H. Among them, motifs A (LVKVGGLIG), B (VAPPDAPLRKY), and C (ALAVDPRIEICM) are general characterizations that exist in all OMTs, whereas motifs D (TSVYPREPEPMKELRELT), E (KLINAKNTMEI), F (PVIQKAGVAHKIEF), G (DFIFVDADKDNY), and H (GDGITLCRR) are specific to CCoAOMT. To date, CCoAOMT family members have been widely identified in diverse species, for example, a total of 6 CCoAOMT genes were presented in the *Populus trichocarpa* genome [37], 7 in *Sorghum bicolor* [38], 21 in *T. aestivum* [39], and 10 in *Vitis vinifera* [25]. However, to the best of our knowledge, a comprehensive survey of StC-CoAOMT gene family members has not been conducted and little functional information exists regarding CCoAOMT in potatoes.

In addition to lignin biosynthesis, CCoAOMT family members have also been reported to be involved in flavonoid biosynthesis. The first CCoAOMT gene associated with the methylation of flavonoids, named *PFOMT*, was identified from *Mesembryanthemum crystallinum*, suggesting that CCoAOMT members participated in the biosynthesis of flavonoids [40]. Unlike other CCoAOMTs that participate in monolignol biosynthe-

sis, PFOMTs accept a wide array of compounds with a vicinal dihydroxyl structure as substrates and exhibit a preference for phenylpropanoids like flavonols and caffeic acid esters [40]. Thus, the CCoAOMT family was further classified into two clades: true CCoAOMT and CCoAOMT-like (PFOMT). Generally, the true CCoAOMT members are involved in lignin biosynthesis in vivo through methylating caffeoyl-CoA, and some members are capable of catalyzing the methylation of flavonoids in vitro [41–43], while the catalytic activity of PFOMT members is mainly manifested in the methylation of flavonols and anthocyanins. Currently, several CCoAOMT-like genes associated with flavonoid and anthocyanin methylation have been reported, such as *VvAOMT* from *V. vinifera* [20], *SlAnthOMT* from *S. lycopersicum* [44], *PpAOMT2* from *Prunus persica* [45], and *CdFOMT5* from *Citrus depressa* [46]. Nevertheless, the potential functions of CCoAOMT family genes on anthocyanin biosynthesis remain unclear in potatoes.

To systematically characterize the potato CCoAOMT gene family, bioinformatics analysis was employed to identify and analyze the CCoAOMT family members, including the chromosome location, duplication event, evolutionary relationship, gene structure, and *cis*-regulatory element. Furthermore, the candidate *StCCoAOMT* gene involved in anthocyanin biosynthesis was identified by RNA-seq and qRT-PCR analysis. This study is conducive to the acknowledgment of CCoAOMT genes and provides a foundation for future research into the function of these genes in potatoes.

2. Materials and Methods

2.1. Plant Materials and Growth Conditions

The plant materials K149-W, K149-Y, and K149-P, representing the white, yellow, and purple tuber flesh, respectively, were introduced from the U.S. National Plant Germplasm System (<https://npgsweb.ars-grin.gov/gringlobal/search>, accessed on 30 May 2021) and cultivated in a glass greenhouse in Anhui Agricultural University. The samples of tuber flesh were collected from potato K149 lines for expression pattern analysis.

Nicotiana benthamiana was planted in plastic pots containing peat soil and vermiculite (1:1) and grown in a climate room, in which the conditions were as follows: 16 h light (23 °C)/8 h dark (18 °C) and relative humidity of 40–60%. Four-week-old *N. benthamiana* was used for the subcellular localization assay.

2.2. Identification of *S. tuberosum* CCoAOMT Genes

The HMM profile of the CCoAOMT conserved domain (PF01596) was retrieved from the InterPro database (<https://www.ebi.ac.uk/interpro/>, accessed on 1 July 2024). The AtCCoAOMT protein sequences of Arabidopsis were downloaded from the TAIR database (<https://www.arabidopsis.org/>, accessed on 1 July 2024). The candidate *StCCoAOMT* protein sequences were identified by HMMER 3.0 software using the HMM profile and Blastp procedure using AtCCoAOMT proteins (e-value < 1×10^{-20}). The common proteins in both HMM and Blastp search were chosen, and the redundant proteins were removed. Subsequently, the candidate *StCCoAOMT* genes were further verified using SMART (<https://smart.embl.de/>, accessed on 5 July 2024), InterPro (<https://www.ebi.ac.uk/interpro/>, accessed on 5 July 2024), and NCBI CD-Search (<https://www.ncbi.nlm.nih.gov/Structure/cdd/wrpsb.cgi>, accessed on 5 July 2024) websites [47]. The physical and chemical properties of *StCCoAOMT* proteins, including the number of amino acids, molecular weight (MW), theoretical pI, grand average of hydropathicity (GRAVY), and instability index (II), were analyzed using the ExpASY online website (<https://web.expasy.org/protparam/>, accessed on 10 July 2024) [48]. The subcellular localization of *StCCoAOMT* proteins was predicted by WoLF PSORT (<https://wolfpsort.hgc.jp/>, accessed on 10 July 2024).

2.3. Chromosomal Distribution and Collinearity Analysis

The information of *StCCoAOMTs* mapped on the chromosomes was extracted from the genome sequence and GFF3 file of 'DM' in Spud DB (<http://spuddb.uga.edu/>, accessed on 12 July 2024). The duplication event of CCoAOMT genes within the 'DM' genome and

the collinearity analysis of the ‘DM’ cultivar associated with *Arabidopsis thaliana*, *Camellia sinensis*, and *S. lycopersicum* genomes were carried out and visualized by TBtools software (v 2.136) [49].

2.4. Phylogenetic Tree, Conserved Motif and Gene Structure Analysis

The CCoAOMT protein sequences of *A. thaliana*, *O. sativa*, and *C. sinensis* were downloaded from TAIR, Phytozome, and NCBI databases, respectively. An unrooted phylogenetic tree was constructed using MEGA 11.0 using the maximum likelihood method with 1000 replicate bootstraps and optimized using the iTOL website (Interactive Tree of Life, <https://itol.embl.de>, accessed on 20 July 2024) [50]. The CCoAOMT protein sequences of *S. tuberosum* were submitted to the online website MEME (<https://meme-suite.org/meme/tools/meme>, accessed on 22 July 2024) for conserved motif analysis [51]. The exon–intron structure was analyzed using the GSDS website (Gene Structure Display Server, <https://gsds.gao-lab.org/>, accessed on 22 July 2024). The integrated graph of the evolutionary tree, conserved motifs, and exon–intron structure was visualized by TBtools software [49].

2.5. Cis-Regulatory Elements Analysis of the StCCoAOMT Promoters

The 2000 bp promoter sequence of *StCCoAOMT* genes was extracted from the *S. tuberosum* genomic file (.gff) and then submitted to the PlantCARE website (<http://bioinformatics.psb.ugent.be/webtools/plantcare/html>, accessed on 24 July 2024) to analyze the *cis*-acting regulatory elements [52]. The heatmap of *cis*-elements in the promoter regions was visualized by TBtools software [49].

2.6. Total RNA Extraction and qRT-PCR Analysis

Total RNA was extracted from potato K149 lines using the RNAPrep Pure Plant Plus Kit (TIANGEN, Beijing, China). The first strand of cDNA was synthesized by the reverse transcription of 1 µg of RNA utilizing the PrimeScript™ first-strand cDNA synthesis kit (TaKaRa, Kyoto, Japan). The qRT-PCR assay was carried out using the SYBR Premix Ex Taq II Kit (Takara, Kyoto, Japan). Each 10 µL of the reaction system consisted of 0.5 µL of cDNA, 0.25 µL of the forward primer, 0.25 µL of the reverse primer, 5 µL of TB Green™ Premix Ex Taq™ II, and 4 µL of RNase-free H₂O. The reaction procedure was as follows: 95 °C for 30 s; 95 °C for 10 s, 60 °C for 20 s, 72 °C for 30 s, and 40 cycles. The relative expression was calculated by the $2^{-\Delta\Delta C_t}$ method. The *StActin* was selected as the housekeeping gene. The gene-specific primers were designed by the NCBI website and are listed in Table S1.

2.7. Gene Cloning and Vector Construction

The cDNA sample of K149-P tuber flesh was utilized as the template for PCR amplification. The full coding sequence of the *StCCoAOMT10* gene was cloned using PrimeSTAR® GXL DNA Polymerase and gene-specific primers. The amplified target fragment was integrated with the linearized pRI101 vector digested with the *Sal* I and *Bam*HI enzymes using the homologous recombination method to generate overexpression vector 35S::StCCoAOMT10-GFP and then transform the positive plasmids into *Agrobacterium tumefaciens* strain GV3101.

2.8. Subcellular Localization of StCCoAOMT10 in Tobacco

The positive *Agrobacterium* clones containing 35S::StCCoAOMT10-GFP and nuclear-localized marker (H₂B-mCherry) were cultured in the liquid Luria–Bertani (LB) medium at 28 °C and resuspended in the infection buffer (10 mM MES, 10 mM MgCl₂, 150 µM acetosyringone) to OD₆₀₀ = 0.8, respectively. Four-week-old *N. benthamiana* leaves were used for the co-injection of the above two suspensions, and the empty vector (35S::GFP) was used as a control. After 48 h, the *Agrobacterium*-inoculated tobacco leaves were cut into 1 × 1 cm sizes for the preparation of samples. The signals of the green fluorescent protein (GFP) and red fluorescent protein (RFP, H₂B-mCherry) of leaves were observed and

photographed by a laser scanning confocal microscope (Leica STELLARIS 5, Mannheim, Germany) [53]. The excitation wavelengths of 488 nm and 580 nm were used for GFP and RFP observation, respectively.

3. Results

3.1. Genome-Wide Identification and Physicochemical Analysis of the CCoAOMT Family in *S. tuberosum*

The StCCoAOMT family member was identified in the *S. tuberosum* (cultivar ‘DM’) genome through BLASTP and HMMER searches. Initially, we obtained 19 putative StC-CoAOMT genes with the BLASTP search and 18 putative StCCoAOMT genes with the HMMER search. Subsequently, 13 unique genes were filtered by CDD, SMART, and InterProScan analyses to remove the false-positive sequences. Eventually, 12 CCoAOMT genes were identified in the potato genome and labeled as StCCoAOMT1–StCCoAOMT12 according to the order of localization on the chromosomes (Table 1).

Table 1. Characterization of StCCoAOMT family members in potato.

Gene Name	Gene ID	Number of Amino Acids	Molecular Weight (kDa)	Theoretical pI	Instability Index	Aliphatic Index	GRAVY	Subcellular Localization
StCCoAOMT1	Soltu.DM.01G047320	248	27.99	5.53	37.62	101.45	−0.227	Cytoplasm
StCCoAOMT2	Soltu.DM.02G028520	242	27.33	5.29	42.1	97.15	−0.251	Cytoplasm
StCCoAOMT3	Soltu.DM.02G028530	175	19.69	5.18	40.75	109.26	−0.045	Cytoplasm
StCCoAOMT4	Soltu.DM.02G028540	242	27.25	5.29	39.05	97.15	−0.244	Cytoskeleton
StCCoAOMT5	Soltu.DM.02G028550	242	27.28	5.3	39.05	97.56	−0.245	Cytoskeleton
StCCoAOMT6	Soltu.DM.03G003400	441	49.72	5.13	42.69	106.37	−0.126	Cytoplasm
StCCoAOMT7	Soltu.DM.04G025040	244	27.57	5.3	37.84	98.73	−0.205	Cytoplasm
StCCoAOMT8	Soltu.DM.04G025050	282	31.76	5.32	46.16	95.11	−0.193	Chloroplast
StCCoAOMT9	Soltu.DM.08G001680	288	32.22	7.08	36.53	97.74	−0.106	Chloroplast
StCCoAOMT10	Soltu.DM.09G025040	234	26.33	5.51	35.93	103.33	−0.118	Cytoplasm
StCCoAOMT11	Soltu.DM.10G014940	245	27.85	5.14	34.38	100.73	−0.271	Cytoplasm
StCCoAOMT12	Soltu.DM.12G013090	123	13.72	4.93	55.56	111.71	−0.031	Cytoplasm

The coding sequence (CDS) lengths of StCCoAOMT genes ranged from 369 to 1323 nucleotides. The length of StCCoAOMT protein sequences varied from 123 to 441 amino acids. The StCCoAOMT proteins had a maximum and minimum molecular weight of 13.72 kilodaltons (kDa) (StCCoAOMT12) and 49.72 kDa (StCCoAOMT6), respectively, and the average molecular weight was 28.22 kDa. The proteins of StCCoAOMT genes had a theoretical pI spectrum of 4.93 (StCCoAOMT12) to 7.08 (StCCoAOMT9). About 58.33% of the StCCoAOMT proteins (7 StCCoAOMTs) were considered stable proteins. The prediction of the grand average of hydropathicity (GRAVY) values demonstrated that all StCCoAOMT proteins are hydrophilic (Table 1). In addition, the prediction of subcellular localization showed that approximately 66.67% of the StCCoAOMT proteins (eight) were located in the cytoplasm region, two in the cytoskeleton (StCCoAOMT4 and StCCoAOMT5), and two in the chloroplast (StCCoAOMT8 and StCCoAOMT9).

3.2. Chromosome Mapping of StCCoAOMT Genes

All StCCoAOMT genes were physically mapped onto eight chromosomes. The StC-CoAOMT genes were not evenly distributed on eight chromosomes in the potato but were densely located in two chromosome regions. Among them, chromosome 2 was the main distribution site, accounting for 33.33% of the total StCCoAOMT genes, followed by chromosome 4, accounting for 16.67% of the total StCCoAOMT genes. Only one StCCoAOMT member was distributed in chromosomes 1, 3, 8, 9, 10, and 12 (Figure 1). There was no correlation between the number of StCCoAOMT genes and the chromosome length. Additionally, an obvious tandem repeat gene cluster was found on chromosome 2. Duplication analysis exhibited that a total of four tandemly duplicated gene (TDG) pairs with six StCCoAOMT genes were found in potato chromosomes (Figure 1, Table S2).

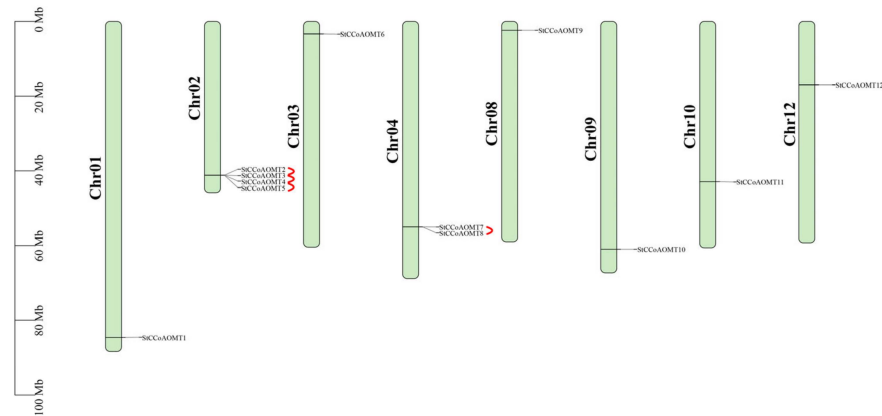


Figure 1. Distribution of *StCCoAOMT* genes in the potato genome.

3.3. Evolutionary Analysis of *StCCoAOMT* Genes

To elucidate the phylogenetic relationship of the CCoAOMT gene family, an unrooted evolutionary tree was constructed based on 35 CCoAOMT proteins, including 7 members from *A. thaliana*, 6 members from *O. sativa*, and 10 members from *C. sinensis* (Figure 2, Table S3). The phylogenetic analysis illustrated that all CCoAOMT proteins were categorized into two clades: group I and group II. Among them, group I contained three subbranches: Ia, Ib, and Ic. *StCCoAOMT1*–*StCCoAOMT5*, *StCCoAOMT11*, and *StCCoAOMT12* were clustered with *AtCCoAOMT1*, *CsCCoAOMT1*, *CsCCoAOMT5*, and *OsCCoAOMT6* into subbranch Ia, which was verified to be involved in lignin biosynthesis. Four *StCCoAOMT*s (*StCCoAOMT6*, *StCCoAOMT7*, *StCCoAOMT8*, and *StCCoAOMT10*) were grouped in subbranch Ib. Except for the CCoAOMTs of *O. sativa*, CCoAOMTs of the other species were not classified into Ic branch, suggesting that subgroup Ic might only exist in monocotyledons. Group II included *StCCoAOMT9*, *CsCCoAOMT4*, *OsCCoAOMT4*, *AtCCoAOMT3*, and *AtCCoAOMT4* and exhibited a distant evolutionary relationship with Group I.

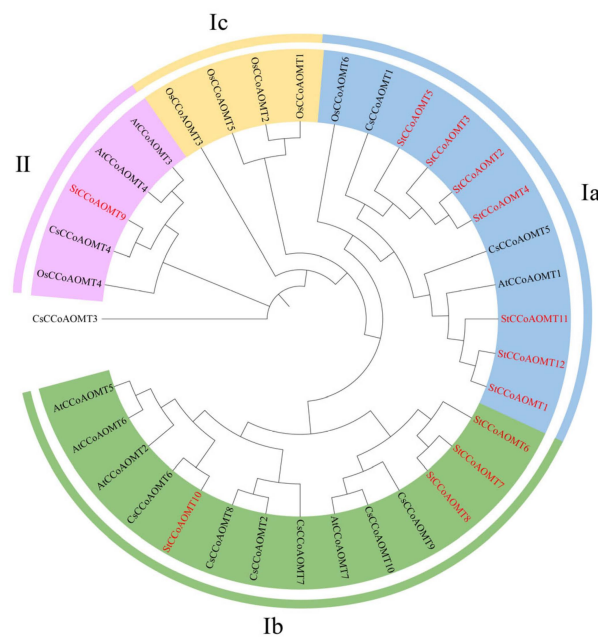


Figure 2. Phylogenetic relationship of CCoAOMTs from *S. tuberosum* and other species. At: *A. thaliana*, Os: *O. sativa*, Cs: *C. sinensis*, St: *S. tuberosum*. The four groups were differentiated with different colors, and CCoAOMTs from potatoes are highlighted with red font.

3.4. Intraspecific and Interspecific Collinearity Analysis of CCoAOMT Genes

Duplication events have vital biological significance in the plant kingdom. To investigate the evolutionary relationships among *StCCoAOMT* genes, the collinearity within the *StCCoAOMT* family was analyzed. The result indicated that only two homologous pairs (*StCCoAOMT1/StCCoAOMT2* and *StCCoAOMT1/StCCoAOMT11*) were identified in the *StCCoAOMT* family (Figure 3A). In addition, the ratios of non-synonymous (Ka) and synonymous (Ks) substitution (Ka/Ks) of segmentally duplicated gene pairs were lower than 1, indicating that the *StCCoAOMT* gene had undergone purifying selection.

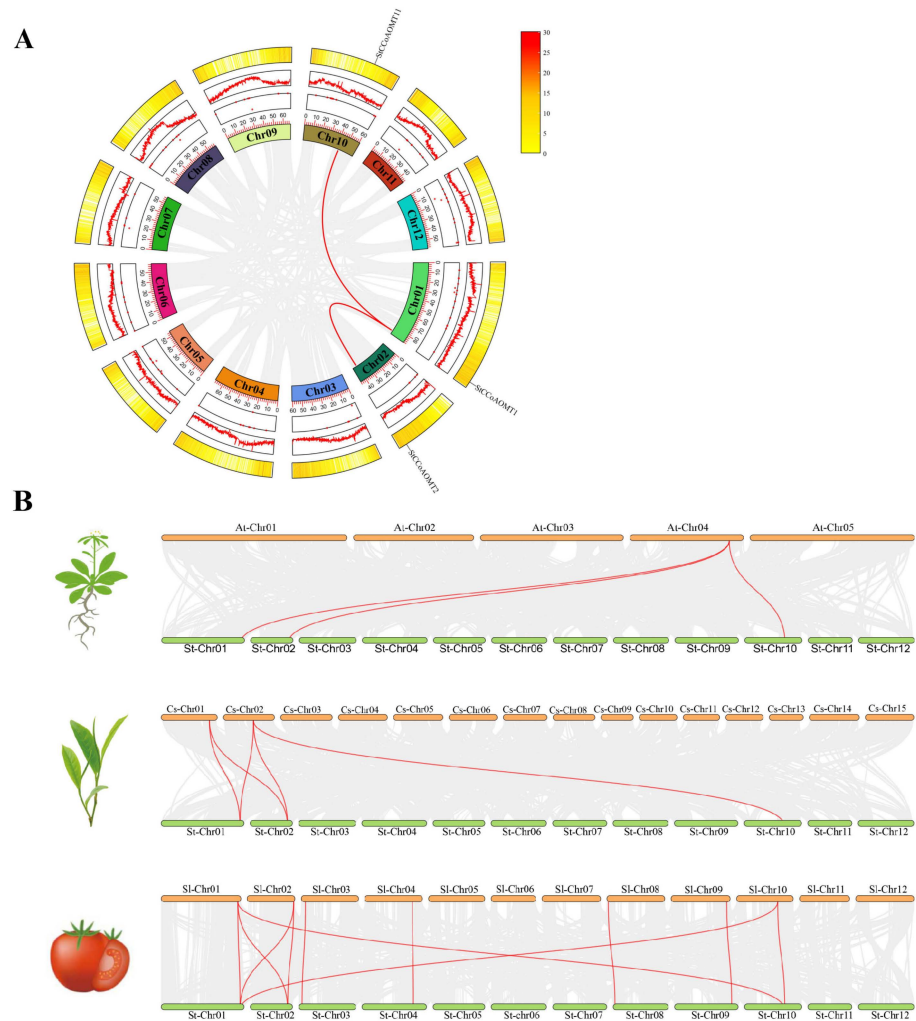


Figure 3. Collinearity analysis of *S. tuberosum* and different species. (A) Intraspecific collinearity analysis of *StCCoAOMT* genes. (B) Evolutionary relationship analysis between *S. tuberosum* to *A. thaliana*, *C. sinensis*, and *S. lycopersicum*. Gray lines represent all syntenic blocks identified between the genomes of different species, and red lines represent the gene pairs with duplicated events.

To further explore the evolutionary relationships of CCoAOMT family members, the interspecies comparative syntenic maps concerning *A. thaliana*, *C. sinensis*, and *S. lycopersicum* were constructed. Interspecific collinearity analysis demonstrated that three *StCCoAOMT* genes displayed syntenic relationships with *AtCCoAOMTs* (*StCCoAOMT1/AtCCoAOMT1*, *StCCoAOMT2/AtCCoAOMT1*, and *StCCoAOMT11/AtCCoAOMT1*). A total of 5 pairs of collinear genes were found between *S. tuberosum* and *C. sinensis*, and 11 pairs of collinear genes were found between *S. tuberosum* and *S. lycopersicum*, with higher homology observed between *S. tuberosum* and *S. lycopersicum* (Figure 3B, Table S4), illustrating *S. tuberosum* had a closer evolutionary relationship with *S. lycopersicum*.

3.5. Conserved Motif Composition and Gene Structure of StCCoAOMT Family Members

To gain further insight into the structural characteristics of StCCoAOMT proteins, the distribution of conserved motifs was predicted using MEME. A total of eight conserved motifs were identified and designated as motifs 1–8 (Figure 4, Figure S1). Members of the StCCoAOMT family had a relatively conserved motif distribution comprising only one AdoMet_Mtases superfamily protein structural domain. The number of conserved motifs varied from two to eight among different StCCoAOMT members and shared similar motif distributions within the same subclass, which is consistent with the phylogenetic tree result. In subgroup Ia, with the exception of StCCoAOMT3 and StCCoAOMT12, all StCCoAOMT proteins contain motifs 1–7. Among them, StCCoAOMT2, StCCoAOMT4, and StCCoAOMT5 contain all motifs. The StCCoAOMT members in subgroup Ib possess motifs 1–6, whereas group II member StCCoAOMT9 only contains motifs 1, 3, 5, and 6. Motif 1 was generally presented in all twelve StCCoAOMT members, demonstrating that it may be critical for the conserved function of StCCoAOMT proteins.

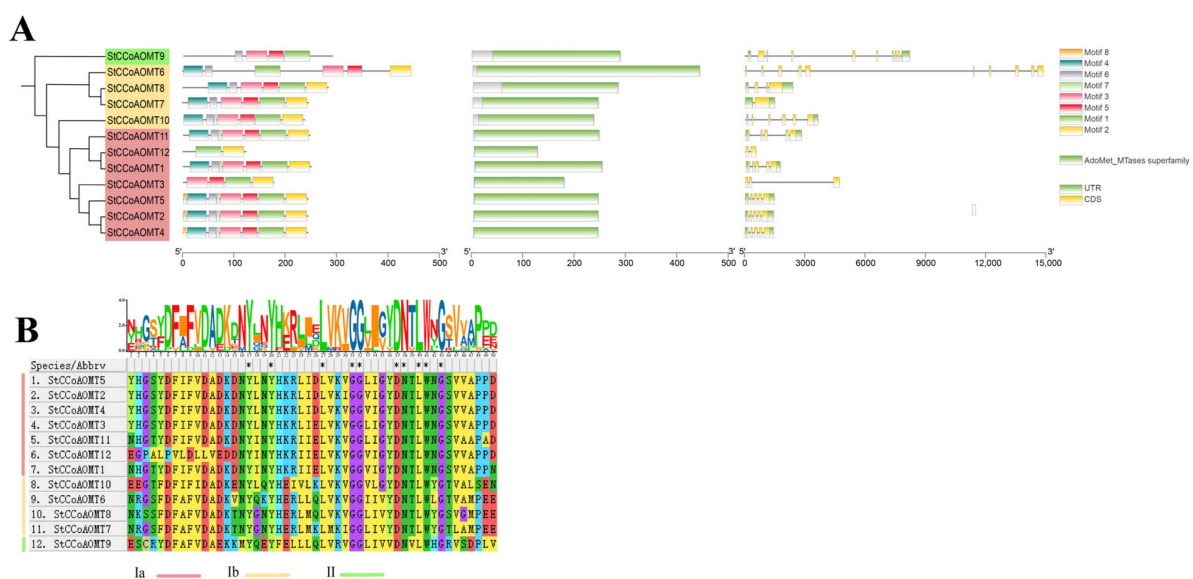


Figure 4. Conserved domain and gene structure analysis. (A) The phylogenetic relationship, conserved motifs, domain distribution, and exon–intron structures of the StCCoAOMTs. (B) The HHM logos of the conserved motif 1 in all StCCoAOMT proteins. The asterisk “*” indicates a highly conserved protein.

In addition, the exon–intron arrangement patterns of StCCoAOMT family members were analyzed. As illustrated in Figure 4A, the exon numbers of StCCoAOMT genes ranged from 2 to 10. The majority of StCCoAOMT members (StCCoAOMT1, StCCoAOMT2, StCCoAOMT4, StCCoAOMT5, StCCoAOMT10, and StCCoAOMT11) possess five exons and four introns, StCCoAOMT3 and StCCoAOMT8 have three exons and two introns, and the gene structure of StCCoAOMT6 and StCCoAOMT9 differed prominently from that of other members featuring ten and nine exons, respectively. Specifically, StCCoAOMT7 and StCCoAOMT12 exhibit a distinct pattern with only two exons. These results uncovered that StCCoAOMTs have diverse structural patterns based on their features and that members categorized into the same subgroup possess similar conserved motifs and exon–intron structures. Thus, we speculated that StCCoAOMT genes within the same clade may share functional similarities.

3.6. Cis-Regulatory Elements Analysis of StCCoAOMT Genes

To investigate the potential function of StCCoAOMT genes, the cis-elements of the 2000 bp promoter sequence were analyzed. Based on their potential functions, these elements can be classified into four types: plant growth and development elements, light-

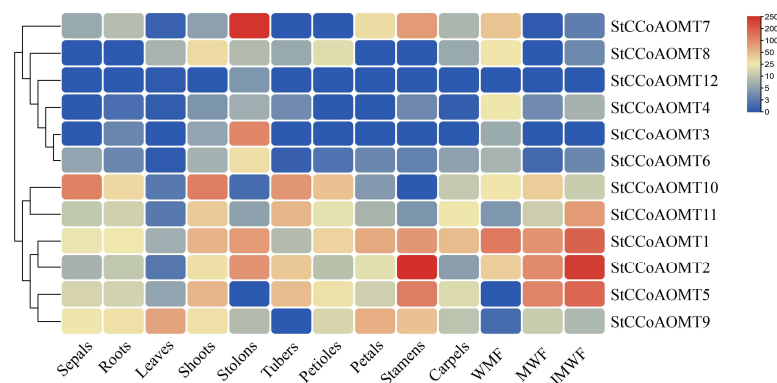


Figure 6. The tissue-specific expression patterns of *StCCoAOMT* genes at different developmental stages of potato. Transcript levels of *StCCoAOMT* gene in sepals, roots, leaves, shoots, stolons, tubers, petioles, petals, stamens, carpels, whole mature flower (WMF), mature whole fruit (MWF), and immature whole fruit (IMWF).

3.8. Identification of Candidate *StCCoAOMT* Gene Involved in Anthocyanin Biosynthesis

Methylation modification is an important step in the biosynthesis of anthocyanins. Given the wide participation of *CCoAOMT* genes in the biosynthesis of secondary metabolites, including flavonoids in plants, we speculated that *StCCoAOMT* members also play pivotal roles in anthocyanin synthesis in potatoes, thereby enhancing their chemical stability. Currently, the key *CCoAOMT* gene and its function in the methylation process of anthocyanins have not yet been systematically investigated and elucidated in potatoes.

To explore the potential members related to the formation of O-methylated flavonoids in potatoes, the expression patterns of *StCCoAOMT* members were analyzed in potato K149 lines with different colors. Expression level analysis discovered that *StCCoAOMT3*, *StCCoAOMT7*, and *StCCoAOMT12* were not expressed or had low expression levels in different lines (Figure 7). The transcript levels of *StCCoAOMT8* and *StCCoAOMT11* in white (K149-W) and purple (K149-P) tubers were relatively higher than those in yellow tubers (K149-Y), and the expression levels were the highest in white tubers. The expression abundance of *StCCoAOMT10* was significantly higher in the tuber-fleashes of the K149-P line with high anthocyanin content than that in the K149-W and K149-Y lines with lower anthocyanin content. In addition, RT-qPCR analysis further revealed that the transcript level of *StCCoAOMT10* gene in all K149 lines with purple tuber flesh (K149-2/8/10/12) was significantly higher than it in white (K149-1/6/16/17) and yellow tuber flesh (K149-7/11/14/18) (Figure 8). Therefore, the *StCCoAOMT10* was considered a key factor affecting the anthocyanin biosynthesis.

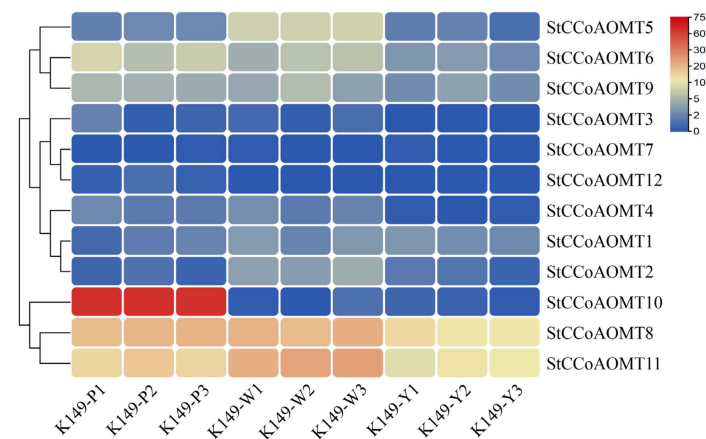


Figure 7. Identification of *StCCoAOMT* genes associated with anthocyanin biosynthesis.

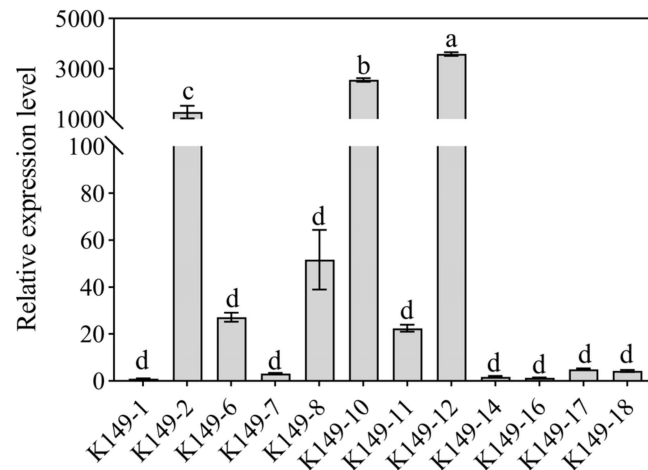


Figure 8. Expression levels of *StCCoAOMT10* gene in different K149 lines. The X-axis shows different potato K149 lines with different tuber flesh colors. White tuber flesh: K149-1/6/16/17; Yellow tuber flesh: K149-7/11/14/18; Purple tuber flesh: K149-2/8/10/12. The lowercase letters represent statistical significance ($p < 0.05$).

3.9. Subcellular Localization of the *StCCoAOMT10* Protein

To detect the distribution of *StCCoAOMT10* in plant cells, the recombinant plasmid of *StCCoAOMT10* fused with the green fluorescent protein (GFP) tag (35S::*StCCoAOMT10*-GFP) was infiltrated into tobacco leaves with nucleus-located mCherry (RFP). As shown in Figure 9, GFP fluorescence of the empty vector (35S::GFP) is located throughout the nucleus and cytoplasm, and the distribution pattern of *StCCoAOMT10* was similar to the empty vector, implicating that *StCCoAOMT10* might participate in the methylation of anthocyanins in the cytoplasm of the plant.

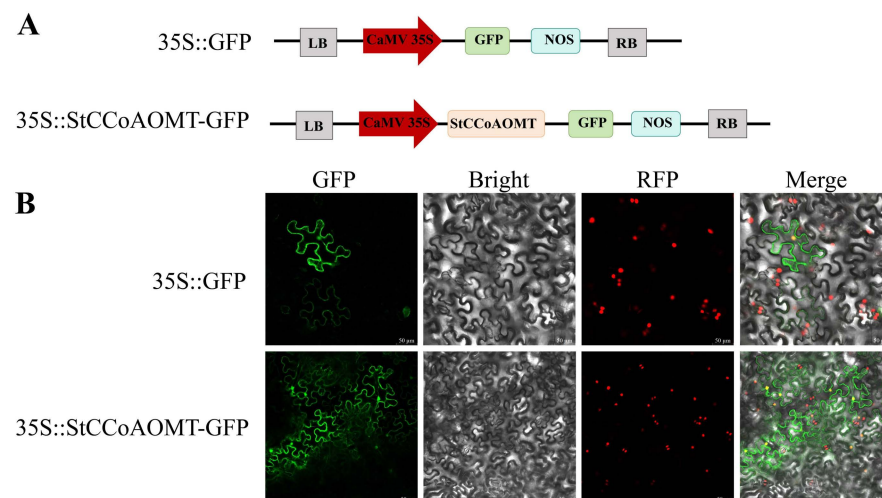


Figure 9. Subcellular localization of *StCCoAOMT10* protein. (A) Illustration of empty vector (35S::GFP) and recombinant constructs (35S::*StCCoAOMT10*-GFP) used in the subcellular localization assay; (B) GFP, Bright, RFP, and Merge represents green fluorescence, light microscopy image, red fluorescence (H₂B-mCherry, nuclear marker), and the combination of fluorescence signals and bright field, respectively. Scale bars = 50 μ m.

4. Discussion

O-methyltransferases (OMTs) are generally involved in the methylation modification of plant secondary metabolites, such as alkaloids, phenylpropanoids, lignins, and flavonoids [54,55]. OMT-mediated methylation enhances the bioactivity, stability, and

solubility of particular natural compounds for adaptation and defense against environmental changes [56,57]. In recent years, the members and functions of OMT genes have been widely identified due to their importance in plant secondary metabolism [25,58]. The Caffeoyl-coenzyme A O-methyltransferase (CCoAOMT) family was classified as class I O-methyltransferase. CCoAOMT family members play a considerable role in catalyzing the O-methylation modification of different compounds in plants, including flavonoids, lignin, and phenylpropionic compounds. CCoAOMT was first isolated in 1989 from suspension cell cultures of *Petroselinum crispum* [59]. Subsequently, many CCoAOMT genes were identified from various plant species, including *P. trichocarpa* [60], *O. sativa* [41], *S. bicolor* [38], and *A. thaliana* [61]. For example, in Arabidopsis, seven CCoAOMTs were identified and classified into three groups. According to previous reports, CCoAOMT proteins can be divided into two categories: the CCoAOMT gene and CCoAOMT-like genes, of which the true CCoAOMT gene represents the orthologous gene with *AtCCoAOMT1* and *OsCCoAOMT1*, also named clade 1a, while CCoAOMT-like genes represent the remaining members, including clade 1b, clade 1c, and clade 2 [38,39]. In this study, a total of 12 *StCCoAOMT* genes were identified in *S. tuberosum* using bioinformatics methods and designated as *StCCoAOMT1*~*StCCoAOMT12*. All *StCCoAOMT* members were irregularly allocated to eight chromosomes. In addition, twelve *StCCoAOMT*s were clustered into three clades based on the phylogenetic relationship, and no *StCCoAOMT* members were clustered into the subbranch 1c, which is in compliance with that of Arabidopsis.

In Arabidopsis, *AtCCoAOMT1* was classified as clade 1a, which has been verified as a regulatory factor that participates in lignin biosynthesis [38,39,62]. At present, *StCCoAOMT1*~5, *StCCoAOMT11*, and *StCCoAOMT12* fall within the same branch as *AtCCoAOMT1*, suggesting these genes may have a potential function in lignin biosynthesis. *AtCCoAOMT6* was confirmed to participate in the biosynthesis of phenylpropanoid polyamine polymers in flower organs [63]. In addition, *AtCCoAOMT7* plays an important role in the biosynthesis of phenylpropane and flavonoid and shows an evident preference for the para methylation of dihydroflavonol and flavanone [63]. Thus, we speculate that *StCCoAOMT6*, *StCCoAOMT7*, *StCCoAOMT8*, and *StCCoAOMT10*, which have a closer phylogenetic relationship with *AtCCoAOMT7*, may be involved in flavonoid biosynthesis. Furthermore, *AtCCoAOMT7* also affects the ferulic acid content in cell walls by regulating S-adenosyl-L-homocysteine (SAH) degradation by binding with SAH hydrolase (SAHH) and S-adenosyl-L-methionine synthases (SAMS) [64].

Our analysis of motif composition and gene structure exhibited that the *StCCoAOMT*s shared similar motif organizations and intron–exon structures in the same clade, suggesting these genes remain relatively conserved during evolutionary processes. Meanwhile, some differences existed in *StCCoAOMT* members of different groups; for example, group 1a has the specific motif 8, indicating functional divergence among *StCCoAOMT* genes. Gene duplication plays a crucial role in gene evolution [65]. The plant CCoAOMT family experienced significant expansion during evolution, potentially to diversify the functions necessary to involve the biosynthesis of secondary metabolites and adapt to the environment. In this study, through collinearity analysis, we identified four pairs of tandem duplicated genes—*StCCoAOMT2/3*, *StCCoAOMT3/4*, *StCCoAOMT4/5*, and *StCCoAOMT7/8*—as well as two pairs of segmental duplicated genes—*StCCoAOMT1/11* and *StCCoAOMT1/12*—suggesting that tandem duplication events play an important role in expanding *StCCoAOMT* family members.

The *cis*-acting elements in the promoter region might act synergistically in accordance with their exclusive functions and growth and development stages, as well as specific conditions [66]. The AC element was generally presented in the promoters of numerous genes that participated in lignin biosynthesis, such as *PAL*, *C4H*, *CAD*, *CCR*, and *CCoAOMT*, indicating that the AC element plays crucial roles in the lignin biosynthetic pathway [67,68]. The MybPlant element in the gene promoter regions of the phenylpropanoid biosynthesis pathway controls lignin biosynthesis by associating with the P-box element [69]. Furthermore, the H-box element was also discovered in the promoters of genes associated

with lignin biosynthesis [70]. The analysis of *cis*-regulatory elements found that lignin-related *cis*-elements were presented in the promoter domains of six *StCCoAOMT* genes (*StCCoAOMT1*, -2, -7, -9, -10, and -11), with most of them containing the P-box motif, suggesting these *StCCoAOMT* genes may be involved in lignin biosynthesis. A wide array of light-responsive elements was identified in the promoters of all *StCCoAOMTs* and hormone-responsive elements in *StCCoAOMT1*, *StCCoAOMT5*, *StCCoAOMT6*, *StCCoAOMT10*, and *StCCoAOMT11* (Figure 5), which may be associated with potato development and anthocyanin synthesis. In addition, several types of stress-responsive elements were also predicted in the *StCCoAOMT* gene promoters, including anoxic-, defense-, drought-, and low-temperature-responsive elements, indicating that the expression of *StCCoAOMTs* is possibly induced by anoxic stress, pathogen infection, drought, and low temperatures.

Flavonoids are a major group of secondary metabolites that are universally accumulated in plants and play extensive roles in phytohormone signaling, pigment accumulation, and defense against different environmental changes based on their various structures [57,71]. Several *CCoAOMT* genes from different plant species were characterized to display substrate preferences for flavonoids, especially anthocyanins [25,58]. In *V. vinifera*, a *CCoAOMT*-like gene was documented to be co-expressed with the methylated anthocyanins and red color in grape berries [72]. The transcript abundance of *AOMT1* was regulated by the MybA protein, and the variation of *AOMT2* structure determined the methylation level of anthocyanins in grapes [21]. Additionally, a *CCoAOMT* member confers a purple color for berry peels by controlling the methylation process of anthocyanins [20,73]. The *SsAOMT5* gene was reported to be involved in the methylation modification of anthocyanins in the peels of wax apples and had a critical effect on red coloration in wax apple peels [74]. However, there are few studies on the biological functionality involving *StCCoAOMT* genes in anthocyanin biosynthesis. Therefore, the transcript abundance of *StCCoAOMT* genes in potato tubers with different coloration was measured. The results showed that the expression levels of the majority of *StCCoAOMT* genes have no significant difference and only *StCCoAOMT10* has a significant expression in K149-P with purple tuber flesh, demonstrating that *StCCoAOMT10* was the primary factor influencing the methylation of anthocyanin. The overexpression or silencing of the *StCCoAOMT10* gene in potatoes should be conducted in the future to deeply understand the roles of the *StCCoAOMT10* gene.

Although the ultimate metabolites of the phenylpropanoid pathway, including anthocyanin biosynthesis, accumulate principally in the vacuoles, the pathways themselves are localized in the cytoplasm, causing speculation that enzymes that participate in the pathways are potentially distributed in the cytoplasm. Previous studies have revealed that the *CsCCoAOMT1* protein from *Citrus reticulata* was localized in the cytoplasm and nucleus [27], while the *VvCCoAOMT4* protein from *V. vinifera* was localized in the membrane and nucleus [25]. At present, the majority of *StCCoAOMT* proteins were predicted to be distributed in the cytoplasm by WoLF PSORT. To verify the subcellular localization of *StCCoAOMTs*, the fusion protein 35S::*StCCoAOMT10*-GFP was constructed and introduced into tobacco leaves. The result demonstrated that *StCCoAOMT10* was a cytoplasmic and nuclear localization protein, indicating that *StCCoAOMT10* might be involved in the methylation of anthocyanins in the cytoplasm of the plant.

5. Conclusions

In conclusion, our work first identified the *CCoAOMT* family members in *S. tuberosum*. The genomic distribution, phylogenetic relationship, conserved motifs composition, and *cis*-regulatory elements of *StCCoAOMT* genes were characterized in detail. The transcript abundances of *StCCoAOMT* genes in various potato tissues were also investigated. In addition, the transcript levels of *StCCoAOMT10* had a significantly positive correlation with anthocyanin biosynthesis in potato tuber flesh. The subcellular localization assay displayed that the *StCCoAOMT10* protein expressed in the cytoplasm and nucleus (Figure 10). This study provided useful information on the evolution of the *CCoAOMT* family in different

plants and shed light on the potential roles of the *StCCoAOMT* genes in regulating potato anthocyanin biosynthesis.

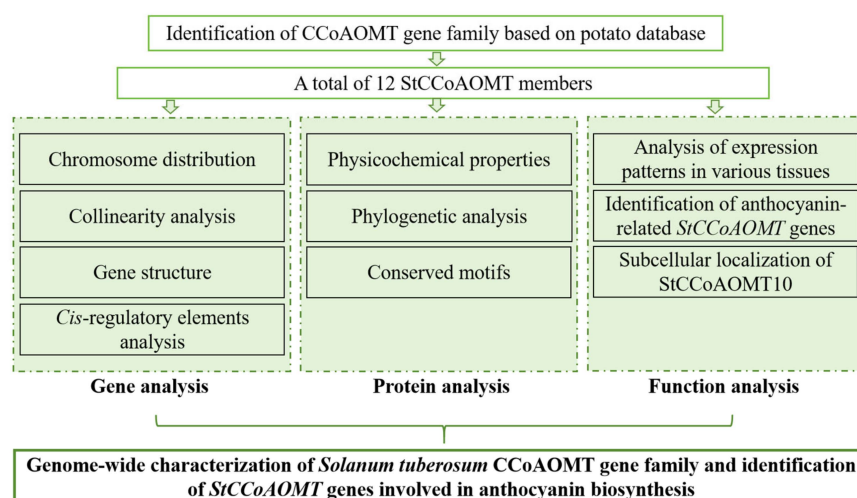


Figure 10. Schematic diagram of experimental design.

Supplementary Materials: The following supporting information can be downloaded at <https://www.mdpi.com/article/10.3390/genes15111466/s1>, Figure S1: Conserved eight motifs of *StCCoAOMT* proteins; Table S1: Primers used in this study; Table S2. Tandem duplicated gene pairs of CCoAOMT gene family in potato; Table S3. The sequences of CCoAOMT protein from different species; Table S4. Syntenic gene pairs between potato and Arabidopsis, *C. sinensis*, tomato.

Author Contributions: Conceptualization, X.Z. and H.H.; data curation, Y.P., S.S., and T.W.; formal analysis, T.W., D.W., and Y.Z.; funding acquisition, H.H. and X.Z.; investigation, Y.P. and S.S.; methodology, Y.P. and T.W.; software, S.S. and J.S.; supervision, Z.L., X.Z., and H.H.; validation, J.S., J.C., and T.Z.; visualization, T.W. and H.H.; writing—original draft, Y.P., S.S., and H.H.; writing—review and editing, Z.L. and X.Z. All authors have read and agreed to the published version of the manuscript.

Funding: This research was funded by the National Natural Science Foundation of China (grant number 32201853), the Anhui Provincial Natural Science Foundation (grant number 2108085QC122, 2308085MC85), and the Natural Science Research Projects of Anhui Province University (grant number KJ2020A0098, KJ2021ZD0013).

Institutional Review Board Statement: Not applicable.

Informed Consent Statement: Not applicable.

Data Availability Statement: The original contributions presented in the study are included in the article and Supplementary Materials, further inquiries can be directed to the corresponding author.

Conflicts of Interest: The authors declare no conflicts of interest.

References

- Liu, M.; Li, Y.; Li, G.; Dong, T.; Liu, S.; Pei, L.; Wang, Q. Overexpression of *StCYS1* gene enhances tolerance to salt stress in the transgenic potato (*Solanum tuberosum* L.) plant. *J. Integr. Agric.* **2020**, *19*, 2239–2246. [\[CrossRef\]](#)
- Birch, P.R.; Bryan, G.; Fenton, B.; Gilroy, E.M.; Hein, I.; Jones, J.T.; Prashar, A.; Taylor, M.A.; Torrance, L.; Toth, I.K. Crops that feed the world 8: Potato: Are the trends of increased global production sustainable? *Food Secur.* **2012**, *4*, 477–508. [\[CrossRef\]](#)
- Qu, G.; Peng, D.; Yu, Z.; Chen, X.; Cheng, X.; Yang, Y.; Ye, T.; Lv, Q.; Ji, W.; Deng, X. Advances in the role of auxin for transcriptional regulation of lignin biosynthesis. *Funct. Plant Biol.* **2021**, *48*, 743–754. [\[CrossRef\]](#) [\[PubMed\]](#)
- Davies, K.M.; Albert, N.W.; Zhou, Y.; Schwinn, K.E. Functions of flavonoid and betalain pigments in abiotic stress tolerance in plants. *Ann. Plant Rev.* **2018**, *1*, 21–62.
- Brunetti, C.; Fini, A.; Sebastiani, F.; Gori, A.; Tattini, M. Modulation of phytohormone signaling: A primary function of flavonoids in plant–environment interactions. *Front. Plant Sci.* **2018**, *9*, 1042. [\[CrossRef\]](#) [\[PubMed\]](#)
- Jansen, M.A. Ultraviolet-B radiation effects on plants: Induction of morphogenic responses. *Physiol. Plantarum.* **2002**, *116*, 423–429. [\[CrossRef\]](#)

7. Erlejan, A.; Verstraeten, S.; Fraga, C.; Oteiza, P. The interaction of flavonoids with membranes: Potential determinant of flavonoid antioxidant effects. *Free Radic. Res.* **2004**, *38*, 1311–1320. [[CrossRef](#)]
8. Stracke, R.; Jahns, O.; Keck, M.; Tohge, T.; Niehaus, K.; Fernie, A.R.; Weisshaar, B. Analysis of PRODUCTION OF FLAVONOL GLYCOSIDES—Dependent flavonol glycoside accumulation in *Arabidopsis thaliana* plants reveals MYB11-, MYB12- and MYB111-independent flavonol glycoside accumulation. *New Phytol.* **2010**, *188*, 985–1000. [[CrossRef](#)]
9. Emiliani, J.; Grotewold, E.; Ferreyra, M.L.F.; Casati, P. Flavonols protect *Arabidopsis* plants against UV-B deleterious effects. *Mol. Plant.* **2013**, *6*, 1376–1379. [[CrossRef](#)]
10. Mutha, R.E.; Tatiya, A.U.; Surana, S.J. Flavonoids as natural phenolic compounds and their role in therapeutics: An overview. *Futur. J. Pharm. Sci.* **2021**, *7*, 25. [[CrossRef](#)]
11. Braun, K.F.; Ehnert, S.; Freude, T.; Egaña, J.T.; Schenck, T.L.; Buchholz, A.; Schmitt, A.; Siebenlist, S.; Schyschka, L.; Neumaier, M. Quercetin protects primary human osteoblasts exposed to cigarette smoke through activation of the antioxidative enzymes HO-1 and SOD-1. *Sci. World J.* **2011**, *11*, 2348–2357. [[CrossRef](#)] [[PubMed](#)]
12. Ramesh, P.; Jagadeesan, R.; Sekaran, S.; Dhanasekaran, A.; Vimalraj, S. Flavonoids: Classification, function, and molecular mechanisms involved in bone remodelling. *Front. Endocrinol.* **2021**, *12*, 779638. [[CrossRef](#)] [[PubMed](#)]
13. Zhao, C.L.; Guo, H.C.; Dong, Z.Y.; Zhao, Q. Pharmacological and nutritional activities of potato anthocyanins. *Afr. J. Pharm. Pharmacol.* **2009**, *3*, 463–468.
14. Li, Z.; Ahammed, G.J. Plant stress response and adaptation via anthocyanins: A review. *Plant Stress.* **2023**, *10*, 100230. [[CrossRef](#)]
15. Kaur, S.; Tiwari, V.; Kumari, A.; Chaudhary, E.; Sharma, A.; Ali, U.; Garg, M. Protective and defensive role of anthocyanins under plant abiotic and biotic stresses: An emerging application in sustainable agriculture. *J. Biotechnol.* **2023**, *361*, 12–29. [[CrossRef](#)]
16. Liu, Y.; Tikunov, Y.; Schouten, R.E.; Marcelis, L.F.; Visser, R.G.; Bovy, A. Anthocyanin biosynthesis and degradation mechanisms in Solanaceous vegetables: A review. *Front. Chem.* **2018**, *6*, 52. [[CrossRef](#)]
17. Lewis, C.E.; Walker, J.R.; Lancaster, J.E.; Sutton, K.H. Determination of anthocyanins, flavonoids and phenolic acids in potatoes. I: Coloured cultivars of *Solanum tuberosum* L. *J. Sci. Food Agric.* **1998**, *77*, 45–57. [[CrossRef](#)]
18. Naito, K.; Umemura, Y.; Mori, M.; Sumida, T.; Okada, T.; Takamatsu, N.; Okawa, Y.; Hayashi, K.; Saito, N.; Honda, T. Acylated pelargonidin glycosides from a red potato. *Phytochemistry* **1998**, *47*, 109–112. [[CrossRef](#)]
19. Azuma, A.; Ban, Y.; Sato, A.; Kono, A.; Shiraishi, M.; Yakushiji, H.; Kobayashi, S. MYB diplotypes at the color locus affect the ratios of tri/di-hydroxylated and methylated/non-methylated anthocyanins in grape berry skin. *Genomes* **2015**, *11*, 31. [[CrossRef](#)]
20. Huguene, P.; Provenzano, S.; Verries, C.; Ferrandino, A.; Meudec, E.; Batelli, G.; Merdinoglu, D.; Cheynier, V.; Schubert, A.; Ageorges, A. A novel cation-dependent O-methyltransferase involved in anthocyanin methylation in grapevine. *Plant Physiol.* **2009**, *150*, 2057–2070. [[CrossRef](#)]
21. Fournier-Level, A.; Huguene, P.; Verriès, C.; This, P.; Ageorges, A. Genetic mechanisms underlying the methylation level of anthocyanins in grape (*Vitis vinifera* L.). *BMC Plant Biol.* **2011**, *11*, 179. [[CrossRef](#)] [[PubMed](#)]
22. Gonzali, S.; Mazzucato, A.; Perata, P. Purple as a tomato: Towards high anthocyanin tomatoes. *Trends Plant Sci.* **2009**, *14*, 237–241. [[CrossRef](#)] [[PubMed](#)]
23. Dubos, C.; Stracke, R.; Grotewold, E.; Weisshaar, B.; Martin, C.; Lepiniec, L. MYB transcription factors in *Arabidopsis*. *Trends Plant Sci.* **2010**, *15*, 573–581. [[CrossRef](#)]
24. Wei, L.; Zhao, X.; Gu, X.; Peng, J.; Song, W.; Deng, B.; Cao, Y.; Hu, S. Genome-wide identification and expression analysis of *Dendrocalamus farinosus* CCoAOMT gene family and the role of DfCCoAOMT14 involved in lignin synthesis. *Int. J. Mol. Sci.* **2023**, *24*, 8965. [[CrossRef](#)]
25. Lu, S.; Zhuge, Y.; Hao, T.; Liu, Z.; Zhang, M.; Fang, J. Systematic analysis reveals O-methyltransferase gene family members involved in flavonoid biosynthesis in grape. *Plant Physiol. Biochem.* **2022**, *173*, 33–45. [[CrossRef](#)]
26. Joshi, C.P.; Chiang, V.L. Conserved sequence motifs in plant S-adenosyl-L-methionine-dependent methyltransferases. *Plant Mol. Biol.* **1998**, *37*, 663–674. [[CrossRef](#)]
27. Liao, Z.; Liu, X.; Zheng, J.; Zhao, C.; Wang, D.; Xu, Y.; Sun, C. A multifunctional true caffeoyl coenzyme AO-methyltransferase enzyme participates in the biosynthesis of polymethoxylated flavones in citrus. *Plant Mol. Biol.* **2023**, *192*, 2049–2066.
28. Gauthier, A.; Gulick, P.J.; Ibrahim, R.K. Characterization of two cDNA clones which encode O-methyltransferases for the methylation of both flavonoid and phenylpropanoid compounds. *Arch. Biochem. Biophys.* **1998**, *351*, 243–249. [[CrossRef](#)]
29. Berim, A.; Hyatt, D.C.; Gang, D.R. A set of regioselective O-methyltransferases gives rise to the complex pattern of methoxylated flavones in sweet basil. *Plant Physiol.* **2012**, *160*, 1052–1069. [[CrossRef](#)]
30. Zhou, J.M.; Seo, Y.W.; Ibrahim, R.K.; Biochemistry. Biochemical characterization of a putative wheat caffeic acid O-methyltransferase. *Plant Physiol. Biochem.* **2009**, *47*, 322–326. [[CrossRef](#)]
31. Kim, B.; Lee, H.; Park, Y.; Lim, Y.; Ahn, J.H. Characterization of an O-methyltransferase from soybean. *Plant Physiol. Biochem.* **2006**, *44*, 236–241. [[CrossRef](#)]
32. Cacace, S.; Schröder, G.; Wehinger, E.; Strack, D.; Schmidt, J.; Schröder, J. A flavonol O-methyltransferase from *Catharanthus roseus* performing two sequential methylations. *Phytochemistry* **2003**, *62*, 127–137. [[CrossRef](#)]
33. Gao, Y.; Wang, X.; Hou, X.; Chen, J. Evolution and Analysis of Caffeic Acid Transferase (COMT) in Seed Plants. *Biochem. Genet.* **2024**, *62*, 1953–1976. [[CrossRef](#)]

34. Ma, G.; Zhang, L.; Seoka, M.; Nakata, A.; Yahata, M.; Shimada, T.; Fujii, H.; Endo, T.; Yoshioka, T.; Kan, T.J. Characterization of a caffeic acid 8-O-methyltransferase from citrus and its function in nobiletin biosynthesis. *Agric. Food Chem.* **2021**, *70*, 543–553. [[CrossRef](#)]
35. Yan, Y.; Sun, S.; Zhao, N.; Yang, W.; Shi, Q.; Gong, B. COMT1 overexpression resulting in increased melatonin biosynthesis contributes to the alleviation of carbendazim phytotoxicity and residues in tomato plants. *Environ. Pollut.* **2019**, *252*, 51–61. [[CrossRef](#)]
36. Do, C.-T.; Pollet, B.; Thévenin, J.; Sibout, R.; Denoue, D.; Barrière, Y.; Lapierre, C.; Jouanin, L. Both caffeoyl Coenzyme A 3-O-methyltransferase 1 and caffeic acid O-methyltransferase 1 are involved in redundant functions for lignin, flavonoids and sinapoyl malate biosynthesis in Arabidopsis. *Planta* **2007**, *226*, 1117–1129. [[CrossRef](#)]
37. Shi, R.; Sun, Y.H.; Li, Q.; Heber, S.; Sederoff, R.; Chiang, V.L. Towards a systems approach for lignin biosynthesis in *Populus trichocarpa*: Transcript abundance and specificity of the monolignol biosynthetic genes. *Mol. Genet. Genom.* **2010**, *51*, 144–163. [[CrossRef](#)]
38. Rakoczy, M.; Femiak, I.; Alejska, M.; Figlerowicz, M.; Podkowinski, J. Sorghum CCoAOMT and CCoAOMT-like gene evolution, structure, expression and the role of conserved amino acids in protein activity. *Mol. Genet. Genom.* **2018**, *293*, 1077–1089. [[CrossRef](#)]
39. Yang, G.; Pan, W.; Zhang, R.; Pan, Y.; Guo, Q.; Song, W.; Zheng, W.; Nie, X. Genome-wide identification and characterization of caffeoyl-coenzyme A O-methyltransferase genes related to the Fusarium head blight response in wheat. *BMC Genom.* **2021**, *22*, 504. [[CrossRef](#)] [[PubMed](#)]
40. Ibdah, M.; Zhang, X.H.; Schmidt, J.; Vogt, T. A novel Mg²⁺-dependent O-methyltransferase in the phenylpropanoid metabolism of *Mesembryanthemum crystallinum*. *Biol. Chem.* **2003**, *278*, 43961–43972. [[CrossRef](#)]
41. Sung, S.H.; Kim, B.-G.; Chong, Y.; Ahn, J.H. Characterization of phenylpropanoid O-methyltransferase from rice: Molecular basis for the different reactivity toward different substrates. *Plant Biol.* **2011**, *54*, 314–320. [[CrossRef](#)]
42. Zhong, R.; Morrison, W.H., II.; Himmelsbach, D.S.; Poole, F.L.; Ye, Z.H. Essential role of caffeoyl coenzyme AO-methyltransferase in lignin biosynthesis in woody poplar plants. *Plant Physiol.* **2000**, *124*, 563–578. [[CrossRef](#)]
43. Zhong, R.; Morrison, W.H., III.; Negrel, J.; Ye, Z.H. Dual methylation pathways in lignin biosynthesis. *Plant Cell* **1998**, *10*, 2033–2045. [[CrossRef](#)]
44. Gomez Roldan, M.V.; Outchkourov, N.; van Houwelingen, A.; Lammers, M.; Romero de la Fuente, I.; Ziklo, N.; Aharoni, A.; Hall, R.D.; Beekwilder, J. An O-methyltransferase modifies accumulation of methylated anthocyanins in seedlings of tomato. *Plant J.* **2014**, *80*, 695–708. [[CrossRef](#)]
45. Cheng, J.; Wei, G.; Zhou, H.; Gu, C.; Vimolmangkang, S.; Liao, L.; Han, Y. Unraveling the mechanism underlying the glycosylation and methylation of anthocyanins in peach. *Plant Physiol.* **2014**, *166*, 1044–1058. [[CrossRef](#)]
46. Itoh, N.; Iwata, C.; Toda, H. Molecular cloning and characterization of a flavonoid-O-methyltransferase with broad substrate specificity and regioselectivity from *Citrus depressa*. *BMC Plant Biol.* **2016**, *16*, 180. [[CrossRef](#)]
47. Jiang, M.; Ren, L.; Lian, H.; Liu, Y.; Chen, H. Novel insight into the mechanism underlying light-controlled anthocyanin accumulation in eggplant (*Solanum melongena* L.). *Plant Sci.* **2016**, *249*, 46–58. [[CrossRef](#)]
48. Gasteiger, E.; Hoogland, C.; Gattiker, A.; Duvaud, S.e.; Wilkins, M.R.; Appel, R.D.; Bairoch, A. Protein identification and analysis tools on the ExPASy server. In *The Proteomics Protocols Handbook*; Springer: Berlin/Heidelberg, Germany, 2005; pp. 571–607.
49. Chen, C.; Wu, Y.; Li, J.; Wang, X.; Zeng, Z.; Xu, J.; Liu, Y.; Feng, J.; Chen, H.; He, Y. TBtools-II: A “one for all, all for one” bioinformatics platform for biological big-data mining. *Mol. Plant.* **2023**, *16*, 1733–1742. [[CrossRef](#)]
50. Wei, K.; Chen, H. Global identification, structural analysis and expression characterization of cytochrome P450 monooxygenase superfamily in rice. *BMC Genom.* **2018**, *19*, 35. [[CrossRef](#)] [[PubMed](#)]
51. Bailey, T.L.; Boden, M.; Buske, F.A.; Frith, M.; Grant, C.E.; Clementi, L.; Ren, J.; Li, W.W.; Noble, W.S. MEME SUITE: Tools for motif discovery and searching. *Nucleic Acids Res.* **2009**, *37*, W202–W208. [[CrossRef](#)] [[PubMed](#)]
52. Lescot, M.; Déhais, P.; Thijs, G.; Marchal, K.; Moreau, Y.; Van de Peer, Y.; Rouzé, P.; Rombauts, S. PlantCARE, a database of plant cis-acting regulatory elements and a portal to tools for in silico analysis of promoter sequences. *Nucleic Acids Res.* **2002**, *30*, 325–327. [[CrossRef](#)] [[PubMed](#)]
53. Li, W.; Wang, T.; Ma, Y.; Wang, N.; Wang, W.; Tang, J.; Zhang, C.; Hou, X.; Hou, H. Ectopic Expression of BcCUC2 Involved in Sculpting the Leaf Margin Serration in *Arabidopsis thaliana*. *Genes* **2023**, *14*, 1272. [[CrossRef](#)]
54. Lam, K.C.; Ibrahim, R.K.; Behdad, B.; Dayanandan, S. Structure, function, and evolution of plant O-methyltransferases. *Genome* **2007**, *50*, 1001–1013. [[CrossRef](#)]
55. Struck, A.W.; Thompson, M.L.; Wong, L.S.; Micklefield, J. S-adenosyl-methionine-dependent methyltransferases: Highly versatile enzymes in biocatalysis, biosynthesis and other biotechnological applications. *ChemInform* **2012**, *13*, 2642–2655.
56. Provenzano, S.; Spelt, C.; Hosokawa, S.; Nakamura, N.; Brugliera, F.; Demelis, L.; Geerke, D.P.; Schubert, A.; Tanaka, Y.; Quattrocchio, F. Genetic control and evolution of anthocyanin methylation. *Plant Physiol.* **2014**, *165*, 962–977. [[CrossRef](#)] [[PubMed](#)]
57. Koirala, N.; Thuan, N.H.; Ghimire, G.P.; Van Thang, D.; Sohng, J.K. Methylation of flavonoids: Chemical structures, bioactivities, progress and perspectives for biotechnological production. *Enzym. Microb. Technol.* **2016**, *86*, 103–116. [[CrossRef](#)] [[PubMed](#)]
58. Widiez, T.; Hartman, T.G.; Dudai, N.; Yan, Q.; Lawton, M.; Havkin-Frenkel, D.; Belanger, F.C. Functional characterization of two new members of the caffeoyl CoA O-methyltransferase-like gene family from *Vanilla planifolia* reveals a new class of plastid-localized O-methyltransferases. *Plant Mol. Biol.* **2011**, *76*, 475–488. [[CrossRef](#)]

59. Pakusch, A.E.; Kneusel, R.E.; Matern, U. S-adenosyl-L-methionine: Trans-caffeoyl-coenzyme A 3-O-methyltransferase from elicitor-treated parsley cell suspension cultures. *Arch. Biochem. Biophys.* **1989**, *271*, 488–494. [[CrossRef](#)]
60. Chen, C.; Meyermans, H.; Burggraeve, B.; De Rycke, R.M.; Inoue, K.; De Vleeschauwer, V.; Steenackers, M.; Van Montagu, M.C.; Engler, G.J.; Boerjan, W.A. Cell-specific and conditional expression of caffeoyl-coenzyme A-3-O-methyltransferase in poplar. *Plant Physiol.* **2000**, *123*, 853–868. [[CrossRef](#)]
61. Chun, H.J.; Lim, L.H.; Cheong, M.S.; Baek, D.; Park, M.S.; Cho, H.M.; Lee, S.H.; Jin, B.J.; No, D.H.; Cha, Y.J. Arabidopsis CCoAOMT1 plays a role in drought stress response via ROS-and ABA-dependent manners. *Plants* **2021**, *10*, 831. [[CrossRef](#)]
62. Wang, P.; Guo, L.; Morgan, J.; Dudareva, N.; Chapple, C. Transcript and metabolite network perturbations in lignin biosynthetic mutants of Arabidopsis. *Plant Physiol.* **2022**, *190*, 2828–2846. [[CrossRef](#)] [[PubMed](#)]
63. Fellenberg, C.; Böttcher, C.; Vogt, T. Phenylpropanoid polyamine conjugate biosynthesis in *Arabidopsis thaliana* flower buds. *Phytochemistry* **2009**, *70*, 1392–1400. [[CrossRef](#)] [[PubMed](#)]
64. Yang, S.X.; Wu, T.T.; Ding, C.H.; Zhou, P.C.; Chen, Z.Z.; Gou, J.Y. SAHH and SAMS form a methyl donor complex with CCoAOMT7 for methylation of phenolic compounds. *Biochem. Biophys. Res. Commun.* **2019**, *520*, 122–127. [[CrossRef](#)] [[PubMed](#)]
65. Zhang, J. Evolution by gene duplication: An update. *Trends Ecol. Evol.* **2003**, *18*, 292–298. [[CrossRef](#)]
66. Wong, D.C.J.; Lopez Gutierrez, R.; Gambetta, G.A.; Castellarin, S.D. Genome-wide analysis of cis-regulatory element structure and discovery of motif-driven gene co-expression networks in grapevine. *DNA Res.* **2017**, *24*, 311–326. [[CrossRef](#)]
67. Leyva, A.; Liang, X.; Pintor-Toro, J.A.; Dixon, R.A.; Lamb, C.J. cis-Element combinations determine phenylalanine ammonia-lyase gene tissue-specific expression patterns. *Plant Cell* **1992**, *4*, 263–271.
68. Lacombe, E.; Van Doorselaere, J.; Boerjan, W.; Boudet, A.M.; Grima-Pettenati, J. Characterization of cis-elements required for vascular expression of the Cinnamoyl CoA Reductase gene and for protein–DNA complex formation. *Plant Cell* **1992**, *4*, 263–271. [[CrossRef](#)]
69. Tamagnone, L.; Merida, A.; Parr, A.; Mackay, S.; Cullanez-Macia, F.A.; Roberts, K.; Martin, C. The AmMYB308 and AmMYB330 transcription factors from Antirrhinum regulate phenylpropanoid and lignin biosynthesis in transgenic tobacco. *Plant Cell* **1998**, *10*, 135–154. [[CrossRef](#)]
70. Patzlaff, A.; McInnis, S.; Courtenay, A.; Surman, C.; Newman, L.J.; Smith, C.; Bevan, M.W.; Mansfield, S.; Whetten, R.W.; Sederoff, R.R. Characterisation of a pine MYB that regulates lignification. *Plant J.* **2003**, *36*, 743–754. [[CrossRef](#)]
71. Winkel-Shirley, B. Flavonoid biosynthesis. A colorful model for genetics, biochemistry, cell biology, and biotechnology. *Plant Physiol.* **2001**, *126*, 485–493. [[CrossRef](#)]
72. Ageorges, A.; Fernandez, L.; Violet, S.; Merdinoglu, D.; Terrier, N.; Romieu, C. Four specific isogenes of the anthocyanin metabolic pathway are systematically co-expressed with the red colour of grape berries. *Plant Sci.* **2006**, *170*, 372–383. [[CrossRef](#)]
73. Giordano, D.; Provenzano, S.; Ferrandino, A.; Vitali, M.; Pagliarani, C.; Roman, F.; Cardinale, F.; Castellarin, S.D.; Schubert, A. Characterization of a multifunctional caffeoyl-CoA O-methyltransferase activated in grape berries upon drought stress. *Plant Physiol. Biochem.* **2016**, *101*, 23–32. [[CrossRef](#)] [[PubMed](#)]
74. Wei, X.; Li, L.; Xu, L.; Zeng, L.; Xu, J. Genome-wide identification of the AOMT gene family in wax apple and functional characterization of SsAOMTs to anthocyanin methylation. *Plant Sci.* **2023**, *14*, 1213642. [[CrossRef](#)] [[PubMed](#)]

Disclaimer/Publisher’s Note: The statements, opinions and data contained in all publications are solely those of the individual author(s) and contributor(s) and not of MDPI and/or the editor(s). MDPI and/or the editor(s) disclaim responsibility for any injury to people or property resulting from any ideas, methods, instructions or products referred to in the content.